

Differential Projections from the Vestibular Nuclei to the Flocculus and Uvula-Nodulus in Pigeons (*Columba livia*)

JANELLE M.P. PAKAN,¹ DAVID J. GRAHAM,¹ ANDREW N. IWANIUK,²
AND DOUGLAS R.W. WYLIE^{1,2*}

¹Centre for Neuroscience, University of Alberta, Edmonton, Alberta, Canada T6G 2E9

²Department of Psychology, University of Alberta, Edmonton, Alberta, Canada T6G 2E9

ABSTRACT

The pigeon vestibulocerebellum is divided into two regions based on the responses of Purkinje cells to optic flow stimuli: the uvula-nodulus responds best to self-translation, and the flocculus responds best to self-rotation. We used retrograde tracing to determine whether the flocculus and uvula-nodulus receive differential mossy fiber input from the vestibular and cerebellar nuclei. From retrograde injections into the both the flocculus and uvula-nodulus, numerous cells were found in the superior vestibular nucleus (VeS), the cerebellovestibular process (pcv), the descending vestibular nucleus (VeD), and the medial vestibular nucleus (VeM). Less labeling was found in the prepositus hypoglossi, the cerebellar nuclei, the dorsolateral vestibular nucleus, and the lateral vestibular nucleus, pars ventralis. In the VeS, the differential input to the flocculus and uvula-nodulus was distinct: cells were localized to the medial and lateral regions, respectively. The same pattern was observed in the VeD, although there was considerable overlap. In the VeM, the majority of cells labeled from the flocculus were in rostral margins on the ipsilateral side, whereas labeling from uvula-nodulus injections was distributed bilaterally throughout the VeM. Finally, from injections in the flocculus but not the uvula-nodulus, moderate labeling was observed in a paramedian area, adjacent to the medial longitudinal fasciculus. In summary, there were clear differences with respect to the projections from the vestibular nuclei to functionally distinct parts of the vestibulocerebellum. Generally speaking, the mossy fibers to the flocculus and uvula-nodulus arise from regions of the vestibular nuclei that receive input from the semicircular canals and otolith organs, respectively. *J. Comp. Neurol.* 508:402–417, 2008. © 2008 Wiley-Liss, Inc.

Indexing terms: optic flow; optokinetic; vestibulocerebellum; mossy fibers; visual-vestibular integration, fluorescent tracers

Information about self-motion arises from both the visual and vestibular systems. The vestibular apparatus includes the semicircular canals and the otolith organs, which are sensitive to head rotation and translation, respectively (Wilson and Melvill Jones, 1979). Gibson (1954) emphasized that vision can also serve as a proprioceptive sense. Because the environment contains numerous stationary visual stimuli, self-motion induces “flowfields” or “optic flow” across the entire retina. Self-rotation results in a rotational flowfield that is opposite to the direction of one’s head rotation, whereas the flowfield resulting from self-translation consists of a *focus of expansion*, which is a point in the direction of translation from which all visual images radiate outward. A *focus of contraction*, a point to which all visual images converge, is created along the axis

of translation but in the direction opposite to the translation vector (Fig. 1B).

Grant sponsor: the Natural Sciences and Engineering Research Council of Canada (NSERC); Grant number: 170363 (to D.R.W.W.) and a graduate fellowship (to J.M.P.P.); Grant sponsor: the Canadian Institute for Health Research (CIHR); Grant number: 69013 (to D.R.W.W.); Grant sponsor: the Alberta Ingenuity Fund; Grant number: a graduate fellowship (to J.M.P.P.); Grant sponsor: the Canada Research Chairs Program (to D.R.W.W.).

*Correspondence to: Douglas R. Wong-Wylie, Ph.D., University of Alberta, Department of Psychology, Edmonton, Alberta, Canada T6G 2E9. E-mail: dwylie@ualberta.ca

Received 24 May 2007; Revised 3 October 2007; Accepted 3 December 2007

DOI 10.1002/cne.21623

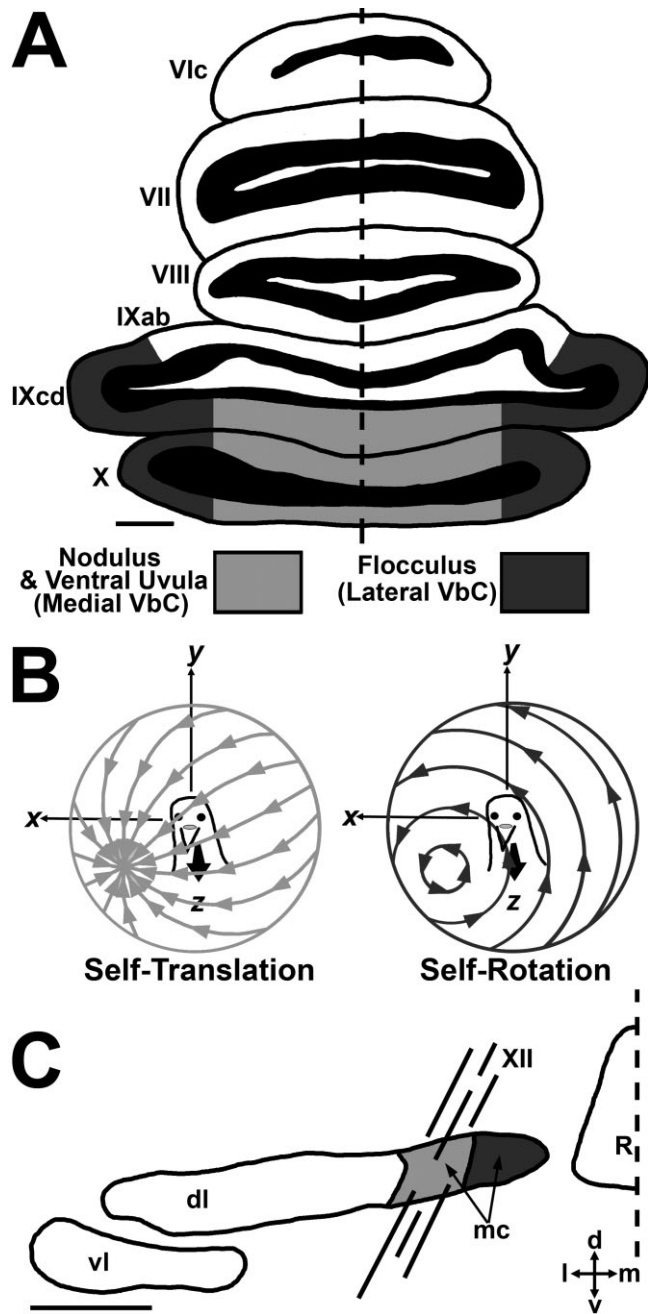


Fig. 1. The rotation and translation olivocerebellar zones of the pigeon vestibulocerebellum (VbC). **A:** A coronal section through the pigeon posterior cerebellum. Purkinje cells in the medial and lateral halves of the VbC (folia IXcd and X) respond to optic flow patterns resulting from self-translation (light gray) and self-rotation (dark gray), respectively. In the rotation zone, both the IXcd and X are collectively referred to as the flocculus. In the translation zone, the IXcd and X are referred to as the uvula and nodulus, respectively (see Nomenclature section in Materials and Methods). **B:** Optic flow patterns resulting from backward self-translation (left) and counterclockwise self-rotation about an axis in the horizontal plane (right). The arrows represent the direction of local image motion in the flowfields. **C:** Areas of the medial column (mc) of the inferior olive that project to rotation and translation zones. The dashed line indicates midline in A and C. m, medial; l, lateral; d, dorsal; v, ventral. For additional abbreviations, see list. Scale bar = 1 mm.

As illustrated in Figure 1, the vestibulocerebellum (VbC) in pigeons can be divided into two general regions based on the complex spike activity (CSA) of Purkinje cells in response to optic flow stimuli. In the medial half, i.e., the ventral uvula and nodulus, Purkinje cells respond to patterns of optic flow that result from self-translation (Wylie et al., 1993, 1998; Wylie and Frost, 1999). In the lateral half, i.e., the flocculus, Purkinje cells respond best to rotational optic flow patterns (Wylie and Frost, 1993). The flocculus and uvula-nodulus receive climbing fiber input from medial and lateral regions of the medial column (mc) of the inferior olive (IO), respectively (Fig. 1; Lau et al., 1998; Wylie et al., 1999b; Crowder et al., 2000). The flocculus and uvula-nodulus also have a differential projection to the vestibular and cerebellar nuclei (Wylie et al., 1999a, 2003a,b).

In vertebrates, there is considerable research demonstrating that the vestibular nuclei project to the VbC. This has been demonstrated for mammals (Voogd et al., 1996; Büttner-Ennever, 1999; Ruigrok, 2003; Büttner and Büttner-Ennever, 2006; Voogd and Barmack, 2006), reptiles (ten Donkelaar, 1998), and frogs (Straka et al., 2001, 2002). Surprisingly, few data are available for birds. Brecha et al. (1980) noted that, after injections of retrograde tracer into the pigeon VbC, retrogradely labeled cells were observed in the vestibular nuclei complex, but, as this was not the focus of their paper, this was the extent of their description. Arends and Zeigler (1991) noted that after injections into the VbC in pigeons, retrograde labeling was found in the superior and descending vestibular nuclei (VeS, VeD). The most extensive study of this projection has been of the developing chick by Diaz and Puelles (2003). After injections into the cerebellum of chick embryos, labeling was most abundant in the VeS, VeD, and medial vestibular nucleus (VeM).

There is also a primary vestibular projection to the VbC. In mammals, the projection from the end organs to the VbC is topographic (Newlands and Perachio, 2003). The flocculus receives a weak primary vestibular input that is mainly from the canals, as opposed to the otolith organs (Kevetter and Perachio, 1986). The primary vestibular projection is very heavy to the uvula and nodulus and arises from all canals and both otolith organs. Generally, the input to the nodulus is heavier from the canals, and the input to the ventral uvula is from the otoliths (Purcell and Perachio, 2001; Voogd and Barmack, 2006). In pigeons, Schwarz and Schwarz (1983) found that all end organs projected throughout the VbC, although the projection was heavier to folium X, as opposed to IXcd. However, they did not find any differences between the projections of the utricle or the canals.

The purpose of the present study was to describe the input from the vestibular nuclei to the VbC in adult pigeons by using retrograde tracing techniques. In particular, we were interested in investigating whether there are differential projections to the flocculus and uvula-nodulus. Furthermore, as the flocculus is involved in analyzing the visual consequences of self-rotation, we predicted that there would be heavier input to the flocculus from those areas of the vestibular nuclei receiving input from the semicircular canals. Likewise, as the uvula-nodulus is involved in analyzing the visual consequences of self-translation, we predicted that there would be heavier input to the uvula-nodulus from those areas of the vestibular

lar nuclei receiving input from the otolith organs (Dickman and Fang, 1996; Schwarz and Schwarz, 1986).

MATERIALS AND METHODS

Surgery and tracer injections

The methods reported herein conformed to the guidelines established by the Canadian Council on Animal Care and were approved by the Biosciences Animal Care and Policy Committee at the University of Alberta. Silver King and Homing pigeons, obtained from a local supplier, were anesthetized by an intramuscular injection of a ketamine (65 mg/kg)/xylazine (8 mg/kg) cocktail. Supplemental doses were administered as necessary. Animals were placed in a stereotaxic device with pigeon ear bars and a beak bar adapter so that the orientation of the skull conformed to the atlas of Karten and Hodós (1967). To access the VbC, the bone surrounding the semicircular canals was removed, as the dorsal surface of the VbC lies within the radius of the anterior semicircular canal. The dura was removed, a glass micropipette (4–5- μ m tip diameter) containing 2 M NaCl was advanced into the flocculus by using a hydraulic microdrive (Fredrick Haern, Bowdoinham, ME), and extracellular recordings of Purkinje cell CSA were made.

The optic flow preference of isolated CSA was identified by moving a large hand-held stimulus (90° × 90°) in various areas of the visual field (after Winship and Wylie, 2006). By using responses to visual stimuli, we could ensure that the electrode was within the flocculus (CSA responsive to rotational optic flow; Wylie and Frost, 1993), or the uvula-nodulus (CSA responsive to translational optic flow; Wylie et al., 1993; Wylie and Frost, 1999). Subsequently, the recording electrode was replaced with a micropipette (20- μ m tip diameter) containing a retrograde tracer: either green or red fluorescent latex microspheres (referred to as Lumafluor; Lumafluor, Naples, FL) or low-salt cholera toxin subunit B (CTB; List Biological Laboratories, Campbell, CA; 1% in 0.1 M phosphate-buffered saline [PBS], pH 7.4). The red and green latex microspheres fluoresce under rhodamine and fluorescein isothiocyanate (FITC) filters, respectively. The fluorescent tracers were pressure injected by using a Picospritzer II (General Valve, Bowdoinham, ME). CTB was injected iontophoretically for 10–15 minutes (+4 μ amps, 7 seconds on, 7 seconds off). After surgery the craniotomy was filled with bone wax, and the wound was sutured. Birds were given an intramuscular injection of buprenorphine (0.012 mg/kg) as an analgesic.

After a recovery period of 2–5 days, the animals were deeply anesthetized with sodium pentobarbital (100 mg/kg) and immediately perfused with either PBS (0.9% NaCl, 0.1 M phosphate buffer) for the animals injected with fluorescent tracers, or PBS followed by 4% paraformaldehyde for all other animals. For the animals injected with fluorescent tracers, the brains were extracted, then flash-frozen in 2-methylbutane, and stored at –80°C until sectioned. Brains were embedded in optimal cutting temperature medium, and 40- μ m coronal serial sections were cut through the brainstem and cerebellum with a cryostat and mounted on electrostatic slides.

Immunohistochemistry

For the animals injected with CTB, the brain was extracted from the skull, embedded in 4% gelatin, and

placed in 30% sucrose in 0.1 M PB for cryoprotection. By using a microtome, frozen serial sections in the coronal plane (40 μ m thick) were collected, and sections were processed for CTB based on the protocol outlined by Wild et al. (1993). Sections were initially rinsed in 0.05 M PBS. They were then washed in a 25% methanol, 0.9% hydrogen peroxide solution for 30 minutes to decrease endogenous peroxidase activity. Sections were rinsed several times in PBS and then placed in 4% rabbit serum with 0.4% Triton X-100 in PBS for 30 minutes.

Tissue was subsequently incubated for 20 hours in the polyclonal primary antibody anti-Cholera toxin, which is grown in goat (0.005%; product 703, List Biological Laboratories), with 0.4% Triton X-100 in PBS. When no injection of CTB is made in the brain, immunohistochemical processing of tissue with this antibody results in no staining. Sections were then rinsed in PBS (several times) and incubated for 60 minutes in 0.16% biotinylated rabbit anti-goat antiserum (Vector, Burlingame, CA) with 0.4% Triton X-100 in PBS. Tissue was rinsed several times with PBS and incubated for 90 minutes in 0.1% ExtrAvidin (Sigma, St. Louis, MO) with 0.4% Triton X-100 in PBS. Subsequent to washes with PBS, the tissue was incubated for 12 minutes in filtered 0.025% diaminobenzidine (DAB) and 0.006% cobalt chloride in PBS. Then 0.005% hydrogen peroxide was added to the DAB solution, and the sections were reacted for up to 6 minutes. The sections were then rinsed several times with PBS and mounted onto aluminum gelatin-coated slides, lightly counterstained with Neutral Red, and coverslipped with Permount.

Analysis of tissue

The sections were examined by using light or fluorescent microscopy as appropriate, with a Leica DMRE equipped with the appropriate fluorescence filters (rhodamine and FITC). To facilitate comparison across cases, the rostral tip of the vestibular complex was identified (i.e., rostral tip of the VeS) and used as a standard. Images were acquired by using a Retiga EXi FAST Cooled mono 12-bit camera (Qimaging, Burnaby BC) and analyzed with OPENLAB imaging software (Improvision, Lexington, MA). Adobe (San Jose, CA) Photoshop was used to compensate for brightness and contrast. To show the distribution of cells throughout the vestibular nuclei, tracings were made from low-power photographs of selected sections (using the FITC filter for the fluorescent cases). The locations of retrogradely labeled cells were marked by examining higher power photographs and while observing the section under the microscope. For the fluorescent cases, the borders of the vestibular nuclei were traced, as they were easy to delineate under the FITC filter because of background autofluorescence. These sections were subsequently stained for Nissl, and the borders were confirmed. To obtain the data for the tables (Tables 2–5) the number of labeled cells was counted from serial sections through the vestibular and cerebellar nuclei at equal intervals, 250 μ m apart. In this quantification, we assume that the number of terminal rosettes per labeled neuron is approximately equal.

In the color figures (Figs. 2, 4, 5), the red has been pseudocoloured magenta, as per Journal policy, to accommodate readers with red-green color blindness.

Nomenclature

As in mammals, the cerebellum in birds is highly foliated but is restricted to a vermis without hemispheres. Folia IXcd (uvula) and X (nodulus), and the rostralateral extension where IXcd and X merge to form the auricle (Au), comprise the VbC. Larsell (1967) considered the lateral extensions of folium IXcd and X as the paraflocculus and flocculus, respectively. In recent years we (Wylie and Frost, 1999; Winship and Wylie, 2003; Wylie et al., 2003a,b) divided the VbC into flocculus, nodulus, and ventral uvula based on function and homology with mammals. Purkinje cells throughout the VbC respond to optokinetic stimulation (e.g., Wylie et al., 1993). In the lateral half of IXcd and X, they respond best to rotational stimuli about the vertical axis (rVA neurons) or a horizontal axis oriented 45° to the midline (rH45 neurons). These responses are essentially identical to those observed in the mammalian flocculus (Graf et al., 1988; Wylie and Frost, 1993). Indeed the zonal organization, climbing fiber inputs, and efferent projections of the rVA and rH45 floccular zones is remarkably similar among mammals and birds (Voogd and Wylie, 2004). Thus, we consider these zones in the lateral half of both IXcd and X as the flocculus. In mammals, a similar phenomenon has occurred: parts of the cerebellum traditionally included in the ventral paraflocculus are now considered part of the “floccular region,” “lobe,” or “complex” (Voogd and Barmack, 2006). More medially, the CSA responds best to translational optic flow (Wylie et al., 1993, 1998; Wylie and Frost, 1999). We refer to the medial half of folia IXcd and X as the uvula and nodulus, respectively or, collectively, as the uvula-nodulus.

For the vestibular and cerebellar nuclei, we generally use the nomenclature of Karten and Hodos (1967), with a few exceptions. According to Karten and Hodos (1967), there are two cerebellar nuclei: the medial and lateral cerebellar nuclei (CbM, CbL), although the CbM can be subdivided further. Arends and Zeigler (1991) identified a third nucleus, the infracerebellar nucleus (Inf), which is difficult to distinguish. The Inf lies ventrolateral to the CbL and dorsal to the dorsolateral vestibular nucleus (VDL; see also Labandeira-Garcia et al., 1989; Arends et al., 1991). The indistinct regions between the CbM, CbL, and the vestibular complex are collectively referred to as the cerebellovestibular process (pcv). According to Karten and Hodos (1967), the vestibular nuclear complex consists of the VeM, the VeS, the descending vestibular nucleus, the lateral vestibular nucleus, pars dorsalis (VeLd) and pars ventralis (VeLv), and the VDL. Most of the VeM consists of parvocellular neurons (VeMpc) and lies dorsal and medial to the stria acoustica, but part of the VeM lies ventral to this fiber bundle. Although traditionally considered part of the VeLv, following the mammalian literature, we refer to this region as the magnocellular VeM (VeMmc; Epema et al., 1988). For convenience, we refer to the rostral and caudal extremes of the VeMpc as the VeMr and VeMc, respectively. Dickman and Fang (1996) considered the VDL to be the dorsal extension of the VeLv. The VDL has been compared with the mammalian group y based on its oculomotor connections.

Dickman and Fang (1996) also identified groups A and B in pigeons, based on earlier studies in chickens (Wold, 1976). In our material, we could not reliably identify these groups A and B; thus, following others (Diaz et al., 2003)

TABLE 1. Single and Double (Both Red and Green Fluorescent Microspheres) Injected Cases

Single injection cases					
Case	Location	Tracer			
Fl#1	Flocculus	CTB			Unilateral
Fl#2	Flocculus	CTB			Unilateral
Fl#3	Flocculus	CTB			Bilateral
UVN#1	Uvula	CTB			Bilateral
UVN #2	Nodulus	CTB			Unilateral
UVN #3	Nodulus	CTB			Unilateral
UVN #4	Uvula	CTB			Bilateral
UVN #5	Nodulus	CTB			Unilateral
UVN #6	Uvula	Green, Lumafluor			Unilateral
UVN #7	Uvula	Green, Lumafluor			Bilateral
UVN #8	Uvula	Green, Lumafluor			Bilateral
Double injection cases					
Case	Red injection	Green injection			
Fl+Fl#1	Left flocculus	Unilateral	Right flocculus	Unilateral	
Fl+Fl#2	Left flocculus	Unilateral	Right flocculus	Unilateral	
Fl+Fl#3	Left flocculus	Unilateral	Right flocculus	Unilateral	
Fl+Fl#4	Right flocculus	Unilateral	Left flocculus	Unilateral	
Fl+Fl#5	Left flocculus	Unilateral	Right flocculus	Unilateral	
Fl+UVN#1	Uvula	Bilateral	Right flocculus	Unilateral	
Fl+UVN#2	Left uvula ¹	Unilateral	Right flocculus	Unilateral	
Fl+UVN#3	Right uvula ²	Unilateral	Right flocculus	Unilateral	
Fl+UVN#4	Left flocculus	Unilateral	Uvula	Bilateral	

¹There was minimal spread into the left flocculus.

²There was some spread of the tracer into the right flocculus.

For abbreviations, see list.

groups A and B are included with the VeS and tangential nucleus (Ta), respectively. The Ta is a collection of large neurons that lies medially to the root of the vestibular nerve. Arends et al. (1991) suggested that the medial Ta corresponds to a group of oculomotor-projecting neurons on the border of the VeM and VeL in mammals (Carleton and Carpenter, 1983; Sato and Kawasaki, 1987). Previous reports suggest that the Ta does not project to the cerebellum (Cox and Peusner, 1990; Arends and Ziegler, 1991).

For the nomenclature of the subdivisions of the inferior olive, we relied on Arends and Voogd (1989). The inferior olive consists of the dorsal and ventral lamella, which are joined medially by the medial column (mcIO). The mcIO projects topographically to the VbC (Wylie et al., 1999b; Crowder et al., 2000).

RESULTS

The results are based on 20 cases in total. There were 11 single injection cases in which CTB (n = 8) or green Lumafluor (n = 3) was injected into either the flocculus or the uvula-nodulus, in addition to 9 double-labeling cases in which red and green Lumafluors were used. Table 1 gives details with respect to the tracers used and the locations of the injections sites for all cases. Retrograde labeling was abundant in the cerebellar and vestibular nuclei (Fig. 2). There were no appreciable differences with respect to the distribution of retrograde labeling between the cases involving the use of CTB as opposed to the Lumafluor, but there were clear differences with respect to the distribution of labeling from injections in the flocculus and uvula-nodulus.

Figure 2A–H shows examples of the retrograde labeling from injections of red and green Lumafluor into the flocculus and uvula-nodulus.

culus and uvula-nodulus. After describing our evaluation of the injection sites, we describe the distribution of mossy fiber inputs to the uvula-nodulus vs. the flocculus separately. Subsequently we will consider the double injection F1+UVN cases, which allow a direct comparison of mossy fiber inputs to the flocculus vs. uvula-nodulus.

Evaluation of the injection sites and olivary labeling

The desire was to restrict injections to either the flocculus or uvula-nodulus. The injections of the Lumafluors were quite easy to delineate, as they had well-circumscribed borders. Figure 2I and J shows injections of green Lumafluor in the uvula and red Lumafluor in the auricle (Au) of the flocculus, respectively. The injections with CTB were more difficult to evaluate as the borders were often indistinct, as is evident with the injection in the flocculus shown in Figure 2K. In particular, with injections in the cerebellar granular layer, the CTB is transported anterogradely along the parallel fibers. Thus, it is difficult to assess the extent to which the injection spread into the molecular layer. In addition to simple observation of the extent of the injection site in coronal sections, we also relied on the location of retrograde labeling in the contralateral mcIO in determining the location of the injection site.

Previous studies have shown that the flocculus and uvula-nodulus receive differential input from the mcIO (Arends and Voogd, 1989; Lau et al., 1998; Wylie et al., 1999; Crowder et al., 2000). The input to the flocculus arises from the most dorsomedial regions of the mcIO, whereas that to the uvula-nodulus arises from the adjacent lateral region. Especially in caudal regions, the fascicles of the 12th cranial nerve separate those olivary neurons projecting to the flocculus and uvula-nodulus. Figure 2D shows labeling in the rostral part of the mcIO from an injection of red tracer into the flocculus and green tracer into the uvula-nodulus. The resultant retrograde labeling is clearly restricted to two separate, but adjacent, regions. The labeling in the inferior olive was critical in determining whether an injection in the uvula-nodulus crossed the midline, as would be evident by bilateral labeling.

Retrograde labeling from injections into the uvula-nodulus

There were eight cases involving single injections into the flocculus (UVN#1–8) in addition to four other double-labeling cases to consider (F1+UVN#1–4; Table 1). Of these 12 cases, 6 were unilateral, and in only 2 did the labeling in the mcIO indicate that there was spread of the tracer into the flocculus (F1+UVN#2 and 3). The amount of labeling through the vestibular and cerebellar nuclei is quantified in Table 2 based on data from four of the unilateral injections and four of the bilateral injections. We also include a quantification of the labeling in the paramedian area (PMA), as there was substantial labeling in this region from injections into the flocculus (see below). From Table 2, it is evident that the distribution of labeling from uvula-nodulus injections was highly consistent between cases and that the labeling was bilaterally symmetric. Across all cases, most of the labeling was found in the VeM (26.7%), VeD (25.1%), and VeS (19.8%). A moderate amount of labeling was also found in the pcv (12.3%), but

less was seen in the VeLv, VDL/INF, ph, CbL, CbM, and PMA.

Drawings of coronal sections from case UVN#4 are used to illustrate the typical pattern of labeling from injections in the uvula-nodulus. Figure 3 shows data from this case in which the injection site was located caudally in the uvula (folium IXcd; Fig. 3A). There were no appreciable differences between cases in which the injection was restricted to the uvula vs. the nodulus. The medial VbC on the left side was targeted, but clearly there was spread across the midline. This was confirmed by the observation that retrograde labeling in the inferior olive was bilateral (Fig. 3B). However, all olivary labeling was found in the lateral mcIO and not the medial portion of the mcIO, indicating that the flocculus was spared. Labeling was found bilaterally in the vestibular and cerebellar nuclei, and because the pattern of labeling was bilaterally symmetric (see also Fig. 5), only the left side of the brain is shown. The labeling in the VeS was restricted to the lateral half, and appeared as a strip spanning the dorsoventral extent (Fig. 3G–J). Caudally this strip persisted such that the lateral half of the pcv was labeled (Fig. 3G). Labeling was found throughout the VeD, but there was a lateral emphasis to this distribution (Fig. 3C–J). Of the labeling in the VeM, most was in the VeMpc, but also in the VeMc, VeMmc, and VeMr (Fig. 3D–J). Some labeling was found in the CbM, with an emphasis in the lateral regions (Fig. 3E–G). A few cells were also found in the VeLv (Fig. 3H,I) but rarely in the VDL, ph, Inf, or CbL. A few cells were seen among the fibers coursing through the medial Ta, where the borders between the Ta, VeLv, and VeD are indistinct (Fig. 3F–H).

Fig. 2. Neurons retrogradely labeled from injections of red and green fluorescent tracers in the vestibulocerebellum (VbC). The "red" injection and labeled cells have been pseudocoloured magenta to accommodate readers with red-green color blindness. **A:** Retrograde labeling in the medial column of the inferior olive (mcIO). The red and green cells are labeled from injections in the flocculus (i.e., rotation zone) and uvula-nodulus (i.e., translation zone), respectively. The white lines indicate the fibers of the 12th cranial nerve (XII). Note that those neurons projecting to the flocculus are found medial to those projecting to the uvula-nodulus. **B:** Retrograde labeling in the extreme rostral portion of the medial vestibular nucleus (VeMr) from an injection into the ipsilateral flocculus. **C:** Retrogradely labeled neurons along the wall of the fourth ventricle from an injection of green tracer into the ipsilateral flocculus. (Red beads were injected into the contralateral uvula-nodulus). **D:** The course this band of cells takes as one moves caudally. The cells line the roof of the brainstem, and there is a clustering of cells in the caudal extreme of the cerebellum-vestibular process (pcv) and the dorsolateral vestibular nucleus (VDL). **E:** Labeling in the superior vestibular nucleus (VeS) from an injection of red tracer into the contralateral uvula-nodulus and green tracer into the ipsilateral flocculus. The green labeling medial to this is located in the extreme rostradorsal margin of the parvocellular medial vestibular nucleus (VeM). **F:** Labeling in the VeS from injections of red tracer into the ipsilateral flocculus and green tracer into the contralateral flocculus. Note that, en masse, the distribution of the ipsi-projecting cells is more medial to that of the contra-projecting cells. **G:** Labeling caudally in the VeD from injections in the uvula-nodulus (red) and flocculus (green). **H:** Labeled cells within the fibers of the medial longitudinal fasciculus (FLM) from an injection in the flocculus. The dashed line in H indicates midline. Arrows indicate double-labeled cells, which appear white. **I:** Injection of green Lumafluor caudally in the uvula (IXcd). **J,K:** Injections of red Lumafluor and cholera toxin subunit B (CTB) in the flocculus, respectively. m, medial; l, lateral. For additional abbreviations, see list. Scale bar = 100 μ m in A–H; 500 μ m in I–K.

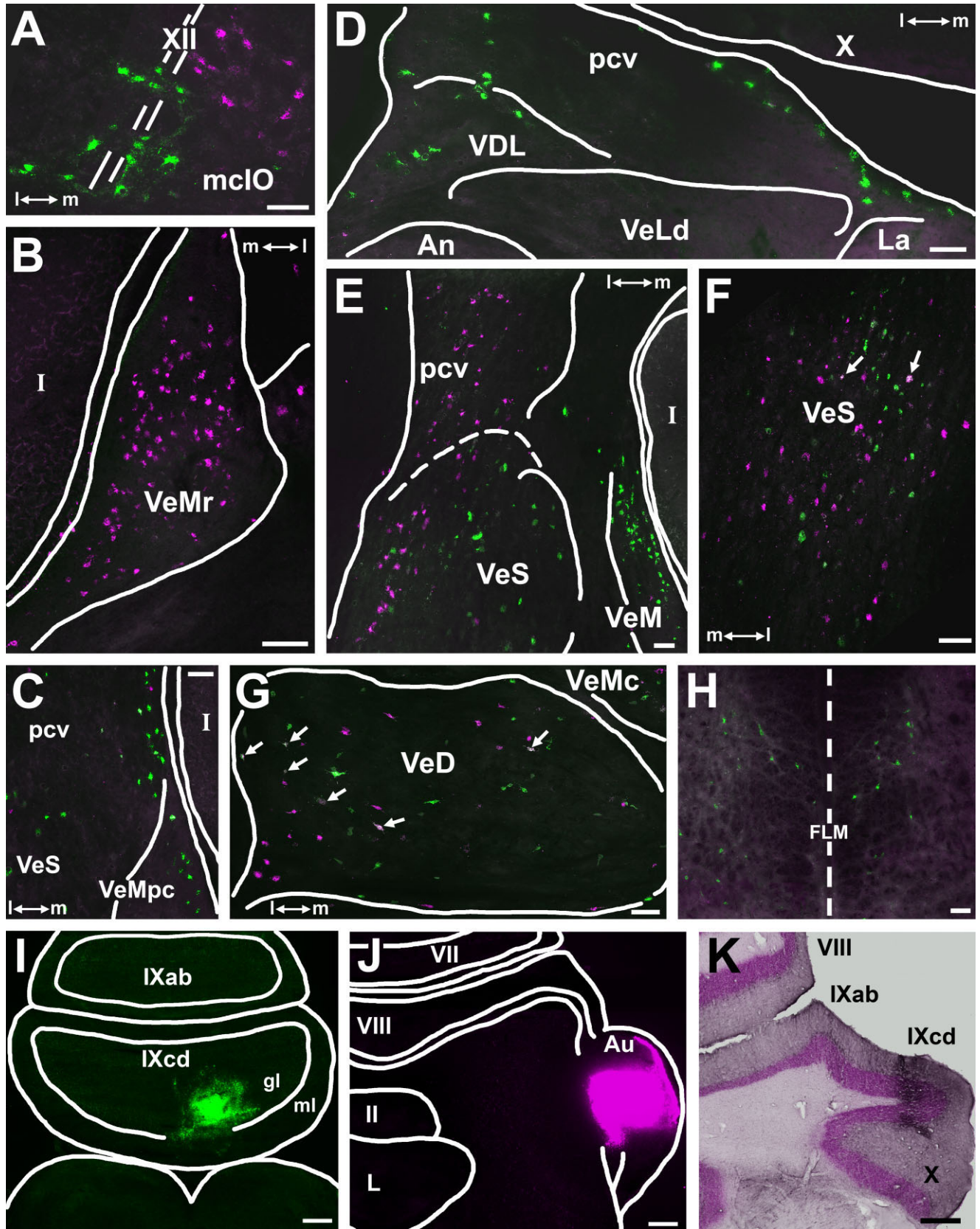


Figure 2

TABLE 2. Distribution of Labeling in the Vestibular and Cerebellar Nuclei From Injections in the Uvula-Nodulus¹

	% Retrogradely labeled cells (mean \pm SEM)		Total ³ Mean \pm S.E.M.
	Ipsilateral ^{2*}	Contralateral ²	
VeM	13.2 \pm 1.7	14.5 \pm 2.7	27.6 \pm 1.9
VeS	7.9 \pm 0.8	10.6 \pm 0.9	19.8 \pm 1.7
pcv	6.2 \pm 1.8	5.4 \pm 0.7	12.3 \pm 1.2
VeLv	1.6 \pm 0.4	2.4 \pm 0.4	3.6 \pm 0.7
VeD	14.2 \pm 1.7	12.0 \pm 1.5	25.1 \pm 1.6
VDL/INF	0.9 \pm 0.2	0.9 \pm 0.1	2.0 \pm 0.2
Ph	0.7 \pm 0.3	1.0 \pm 0.4	1.3 \pm 0.3
CbM	2.1 \pm 0.8	2.5 \pm 0.4	5.2 \pm 0.7
CbL	0.2 \pm 0.2	0	0.2 \pm 0.1
PMA	1.7 \pm 0.7	2.1 \pm 0.8	2.9 \pm 0.8
Total	48.6 \pm 2.0	51.4 \pm 2.0	

¹The percents are shown for the nuclei ipsilateral (I) and contralateral (C) to the injection site, for four cases. A bilateral total is also shown for each nucleus. For abbreviations, see list.

²Based on data from four unilateral injections.

³Based on data from eight cases (four unilateral injections and four bilateral injections).

Retrograde labeling from injections into the flocculus

The pattern of retrograde labeling from injections into the flocculus is based on 17 injections from 12 cases: three cases with unilateral injections of CTB (cases Fl#1–3), five double injection cases in which red and green Lumafluor were injected on opposite sides of the brain (Fl+Fl#1–5), and four double injection cases in which an injection in the flocculus was paired with an injection in the uvula-nodulus (cases Fl+UVN#1–4; Table 1). The amount of labeling through the vestibular and cerebellar nuclei is quantified in Table 3 for eight flocculus injections. The pattern of labeling from all cases was highly consistent. As opposed to the injections in the uvula-nodulus, which resulted in bilaterally symmetric labeling, from the flocculus injections, most of the labeling was found on the side of the brain ipsilateral to the injection site (65.5%). By far the most abundant labeling was found in the ipsilateral VeM (25.7%). Much less labeling was seen in the contralateral VeM (4.4%). A moderate amount of labeling was also seen in the ipsilateral pcv (10.9%, compared with 4.2% in the contralateral pcv) and bilaterally in the VeS (17.4% total). The VeD also contained a moderate amount of labeling, with slightly more on the ipsilateral side (9.4% vs. 5.9%). A moderate amount of labeling was also seen bilaterally in the PMA (15.6% total).

Drawings of coronal sections from case Fl+Fl#3 are shown in Figure 4. Red tracer was injected into the right flocculus, and green was injected in the left flocculus (Fig. 4B–G). On the left side, the injection included both the IXcd and X, whereas on the right side, the injection was mostly in the IXcd. Both injections extended rostrally into the auricle (Fig. 4F,G). The olivary labeling was confined to the dorsomedial region of the mcIO, as expected (Fig. 4A). The heavy labeling in the ipsilateral VeM was concentrated in the rostral VeMpc (VeMr; Fig. 4H,I; see also Fig. 2B,E). The remainder of the VeM labeling was mostly in the caudal parts of the VeMpc, extending into the VeMc (Fig. 4C,D). This labeling was bilateral, but more was found ipsilateral to the injection. There was little labeling in the ipsilateral VeMmc, and surprisingly little in the ph (Fig. 4D–F). Heavy labeling was observed in the medial two-thirds of the VeS (Fig. 4G,H). This labeling was bilat-

eral, but it was clear that the distribution of cells labeled contralateral to the injection site was slightly lateral to that labeled ipsilateral to the injection site (Fig. 4G,H; see also Fig. 5I). Dorsal to the nucleus laminaris, a rather dense band of cells was labeled in the wall of the fourth ventricle ipsilateral to the injection (Fig. 4F,G; see also Fig. 2B). This band of labeling appeared to be continuous with those cells in the extreme dorsal region of the VeMr (Fig. 4H) and continued caudally and laterally along the roof of the brainstem (Fig. 4F,G; see also Fig. 2D).

Many of these cells could be ascribed to the pcv, dorsal to the extreme caudal point of the CbL (Fig. 4F), whereas others were found within the caudal aspect of the VDL (Fig. 4E; see also Fig. 2D). Labeling was found throughout the VeD, although there was a paucity of labeling in the ventrolateral margin (Fig. 4C,D; see also Fig. 2G). More of the labeling in the VeD was ipsilateral to the injection. Caudally, there was moderate labeling bilaterally in the paramedian region, adjacent to the medial longitudinal fasciculus (FLM; Fig. 4B–D). Many of these cells were within the fascicles of the FLM (Fig. 2H) and were clearly caudal to the abducens nucleus, but did not extend as far as the nucleus of the hypoglossal nerve. There were very few labeled cells in the CbM, CbL, VeLv, Ta, and Inf.

Individual cells projecting bilaterally to the flocculus

In cases involving injections of different colors of fluorescent tracer into the flocculus on opposite sides of the brain (i.e., cases Fl+Fl#1–5), the number of double-labeled cells (indicating individual neurons collateralizing and innervating the flocculus bilaterally) was quantified for two cases in Table 4. Expressed as a percentage of the lower total, only 11.3% and 6.2% of the cells were double-labeled in these cases. Double-labeled cells were found in the VeM, VeS (Fig. 2F), pcv, VeD, and PMA. However, it only in the ph was a substantial proportion of cells double-labeled in both cases (6 of 21, 5 of 14).

Direct comparisons of labeling from injections into the flocculus vs. uvula-nodulus

To compare the pattern of retrograde labeling directly from injections in the flocculus vs. the uvula-nodulus, there were four cases in which different colors of fluorescent tracer were injected in the flocculus and uvula-nodulus (Fl+UVN#1–4; Table 1). In Figure 5, representative data are shown from case Fl+UVN#2, in which green tracer was injected into the right flocculus (Fig. 5J,K), and red tracer was injected into the left uvula-nodulus (Fig. 5D–H). In the inferior olive, green retrogradely labeled cells were found medially in the left mcIO, indicating that this injection spared the uvula-nodulus. Cells retrogradely labeled red were densely packed laterally in the right mcIO among the fibers of the 12th cranial nerve, consistent with an injection in the medial VbC. However there were a few labeled cells more medially in the mcIO, indicating that there was some spread of the injection laterally into the flocculus. As there was not heavy labeling in the VeMr typical of flocculus injections (e.g., Fig. 5J,K, green cells), we concluded that the encroachment of the red injection on the flocculus was minimal. There were a few red cells labeled caudally in the left IO (Fig. 5B), indicating that there was some spread of the

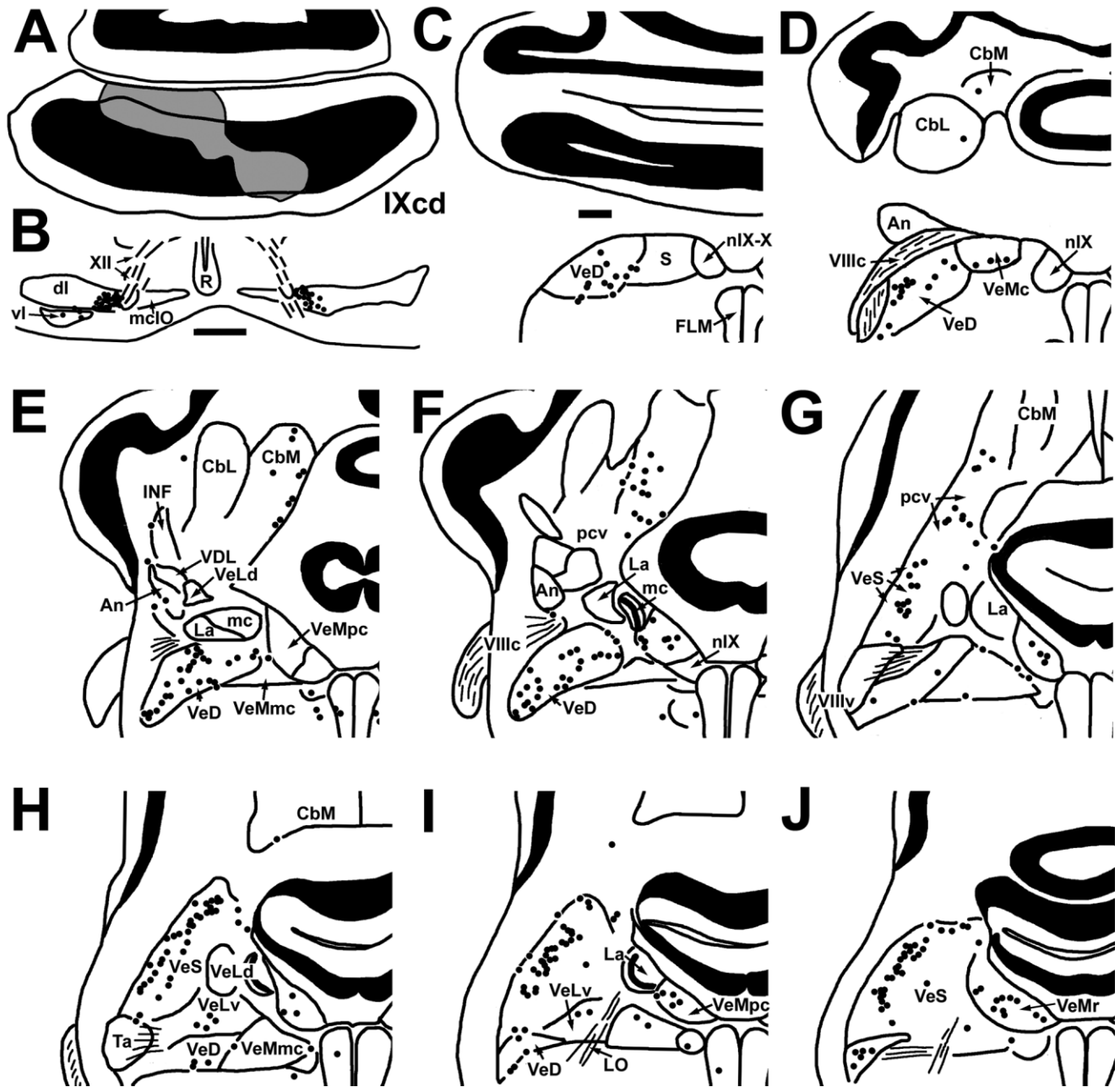


Fig. 3. Retrograde labeling in the vestibular nuclei, cerebellar nuclei, and reticular formation from a CTB injection in the uvula of the medial vestibulocerebellum (VbC). Drawings of coronal sections, caudal to rostral, illustrate the extent of the injection site (A, shaded gray), the labeling in the inferior olive (B), and the extent and distribution of labeling in the vestibular and cerebellar nuclei (C–J). Each

dot represents the location of a retrogradely labeled neuron. As the injection was bilateral, and there were no appreciable differences between labeling on the right and left sides of the brain, only the left side is shown. C–J are approximately 300 μ m apart. For abbreviations, see list. See text for a detailed description. Scale bar = 0.5 mm in B (also applies to A, D–J).

injection across the midline. Thus, this injection was by and large a unilateral injection in the uvula-nodulus contralateral to the green injection in the flocculus.

The distribution of retrogradely labeled cells from the uvula-nodulus and flocculus injections was highly similar to that observed in Figures 3 and 4, respectively. This case effectively offers a direct comparison of the differences between the uvula-nodulus and flocculus with respect to

the pattern of labeling and is representative of the four cases. Rostrally, in the ipsilateral VeMr, labeling was heavy from the flocculus injection (Fig. 5J,K). More caudally in the VeM, there was bilateral labeling from both injections but generally more labeling from the uvula-nodulus injection (Fig. 5E–I). In the VeS, those cells labeled from the flocculus and uvula-nodulus were located in the medial and lateral VeS, respectively. Especially in

TABLE 3. Distribution of Labeling in the Vestibular and Cerebellar Nuclei From Injections in the Flocculus¹

	% Retrogradely labeled cells (mean \pm SEM)	
	Ipsilateral	Contralateral
VeM	25.7 \pm 2.1	4.4 \pm 1.1
VeS	8.5 \pm 0.8	8.9 \pm 1.2
pcv	10.9 \pm 1.3	4.2 \pm 0.8
VeLv	0.6 \pm 0.1	0.7 \pm 0.2
VeD	9.4 \pm 1.1	5.9 \pm 0.6
VDL/INF	1.4 \pm 0.3	0.4 \pm 0.1
Ph	1.2 \pm 0.4	1.2 \pm 0.3
CbM	0.4 \pm 0.2	0.4 \pm 0.2
CbL	0	0
PMA	7.3 \pm 1.1	8.3 \pm 1.5
Total	65.5 \pm 1.5	34.5 \pm 1.5

¹The percents are shown for the nuclei ipsilateral (I) and contralateral (C) to the injection site, for eight flocculus injections. For abbreviations, see list.

the VeS ipsilateral to the flocculus, there was little overlap in this regard (Fig. 5J; see also Fig. 2E). The medial-lateral segregation of cells labeled from the flocculus and uvula-nodulus continued dorsally into the pcv, and the red cells labeled from the uvula-nodulus also extended into the lateral margin of the CbM (Fig. 5J,K).

There was more labeling in the VeLv from the uvula-nodulus injection (Fig. 5G,H), consistent with the quantitative data presented in Tables 2 and 3. In the VeD, labeling was heavier from the uvula-nodulus compared with that to the flocculus. There were slight biases in these distributions. Generally, the labeling from the uvula-nodulus was more lateral than that from the flocculus (Fig. 5D–H). This was most apparent in the ventrolateral extreme of the VeD, where labeling was almost exclusively from the uvula-nodulus (Fig. 5D–F; see also Fig. 2G). Finally, in the paramedian region adjacent to the FLM, there was clearly more labeling from the flocculus injection (Fig. 5D–F).

Individual cells projecting to the flocculus and uvula-nodulus

From the cases involving injections of red and green Lumafluor into the flocculus and uvula-nodulus, some double-labeled cells were observed in the vestibular and cerebellar nuclei. We quantified this for cases F1+UVN#1, 3, and 4 in Table 5. Case F1+UVN#2 was excluded from this analysis because there was spread of the uvula-nodulus injection into the ipsilateral flocculus, indicated by numerous double-labeled cells in the medial mcIO and VeMr. Expressed as a percentage of the lower total, only 15.7, 6.3, and 7.4% of the cells were double-labeled in these three cases (average = 9.8%). The double-labeled cells did not appear to be localized to particular regions within cases or to have a consistent distribution across cases. They were found in all the sites of substantial labeling: the VeM (7–22%), VeS (2–22%), pcv (6–22%), VeD (8–20%; Fig. 2G), and PMA (2–26%). Thus, we conclude that only a minority of cells project to both the flocculus and uvula-nodulus.

DISCUSSION

We have shown that the regions of the pigeon VbC that contain cells responsive to translational and rotational optic flow, i.e., uvula-nodulus and flocculus, receive differential projections from the vestibular and associated nu-

clei. Generally, the projection to the flocculus was stronger from the ipsilateral side by a margin of 2 to 1, whereas the input to uvula-nodulus was equal from the ipsi- and contralateral sides. The differential projection was most distinct in the VeS. Retrogradely labeled cells were found in the medial half of the VeS after injections into the flocculus and in the lateral half after injections into the uvula-nodulus. A similar pattern was observed in the VeD, although there was considerable overlap. In the VeM, from injections in the flocculus, heavy labeling was observed mainly in the VeMr. More caudal areas of the VeM project to both the uvula-nodulus and flocculus, with a heavier projection to the uvula-nodulus.

Comparison with mammals

There are few studies on the vestibulocerebellar projections in birds, but the results of the present study and that of Diaz and Puelles (2003) suggest that the projection is highly conserved. Generally, the vestibulocerebellar projection originates mainly in the VeS, VeD, and VeM in birds, reptiles (ten Donkelaar, 1998), frogs (Straka et al., 2001, 2002), and mammals (Voogd et al., 1996; Büttner-Ennever, 2000; Ruigrok, 2003; Büttner and Büttner-Ennever, 2006; Voogd and Barmack, 2006).

The question of differential projections to the flocculus vs. uvula-nodulus in mammals was addressed directly by Epema et al. (1990). They used double fluorescent retrograde techniques and found that the projections to the uvula-nodulus were quite similar to that of the projection to the flocculus in rabbits. The origin of the projections included the central VeS, the rostral VeM, and caudal portions of both the VeD and VeM. By using CTB as a retrograde tracer in rats, Ruigrok (2003) basically confirmed these results. The projection to the nodulus was mainly from the VeMpc (~45%) and ph (~15%) but also included the VeS and VeD. Most labeled cells from injections into the flocculus were also in the VeM (~20%), and others were observed in the VeD and VeS. However, a differential projection from the vestibular nuclei to the uvula-nodulus vs. flocculus akin to what we observed in the pigeon was not seen in rabbits by Epema et al. (1990). The only exception may be the fact that group X in rabbits projected exclusively to the uvula-nodulus but not the flocculus. We did not distinguish group X in pigeons, but in the lateral margin of the VeD, which is where group X resides in mammals, there was heavier labeling after injections in the uvula-nodulus compared with the flocculus (Figs. 2G, 3E,F, 5E,F).

Epema et al. (1990) found that few neurons were double-labeled after paired injections of retrograde tracers into the flocculus and uvula-nodulus in rabbits (2–12%). This is similar to what we found in the present study (6–16%). Also common to the two studies, the double-labeled cells were not localized to any particular region(s), rather, the distribution of the double-labeled cells was similar to that of single-labeled neurons.

The flocculus in pigeons and mammals seems virtually identical, based on function and connectivity (Voogd and Wylie, 2004). As in pigeons, the mammalian flocculus consists of neurons that respond best to rotational optic flow (i.e., rVA and rH45 neurons; Graf et al., 1988; Wylie and Frost, 1993) arranged in parasagittal zones (Tan et al., 1995; Winship and Wylie, 2003). Moreover, the efferent projection of the zones and the topography of the climbing fiber inputs are quite similar (Ruigrok et al.,

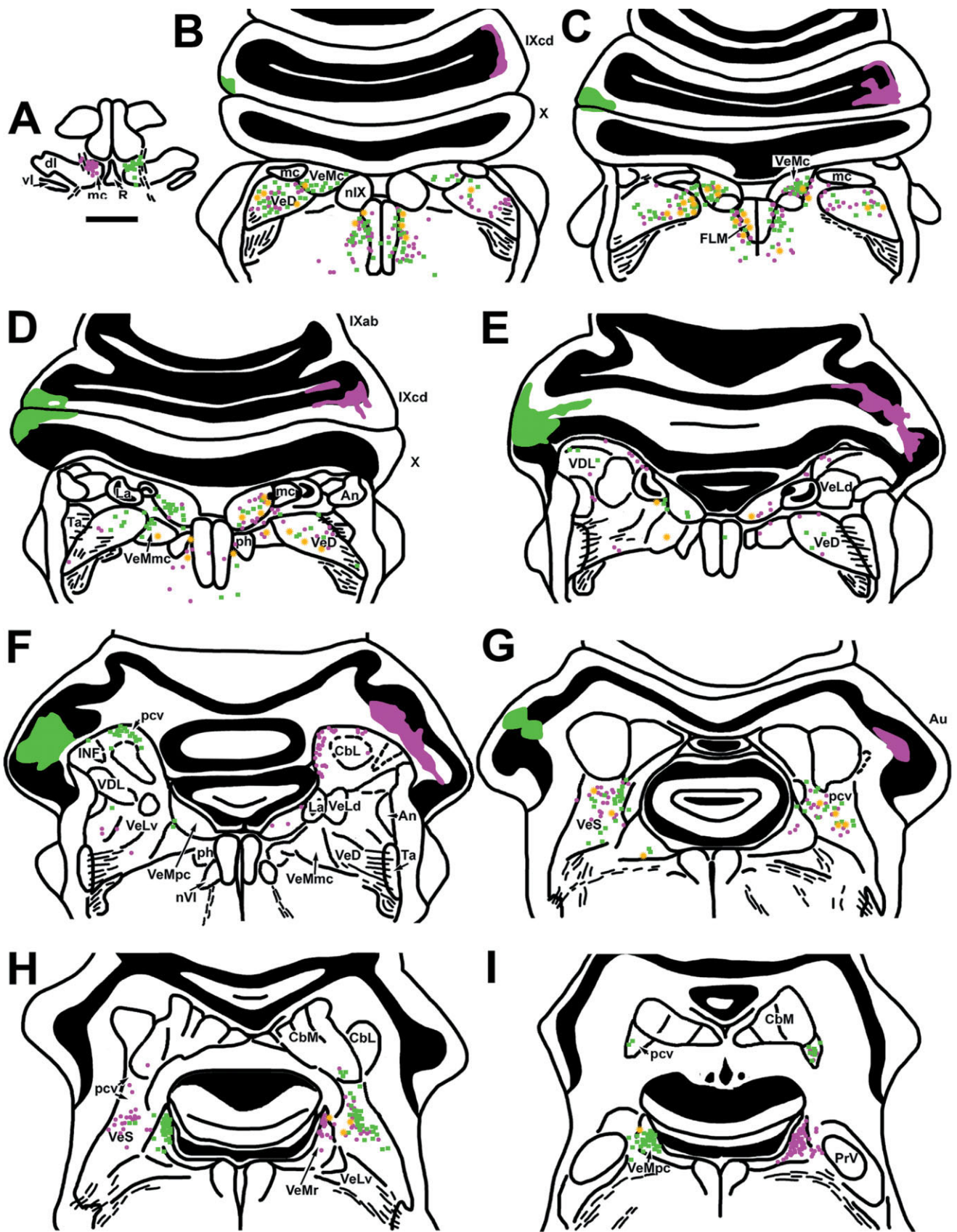


Fig. 4. Retrograde labeling in the vestibular nuclei, cerebellar nuclei, and reticular formation from injections in the flocculus. Drawings of coronal sections, caudal to rostral, illustrate the extent of the injection site (B–G, red and green shading), the labeling in the inferior olive (A), and the extent and distribution of labeling in the vestibular and cerebellar nuclei (B–I). Each shape represents the location of a retrogradely labeled cell and is color-coded

to the injection site (green squares and red circles; the “red” injection and labeled cells have been pseudocoloured magenta to accommodate readers with red-green color blindness). Double-labeled cells obtained from the adjacent section are shown as orange stars. B–I are approximately 350 μ m apart. For abbreviations, see list. See text for a detailed description. Scale bar = 1 mm in A (applies to A–I).

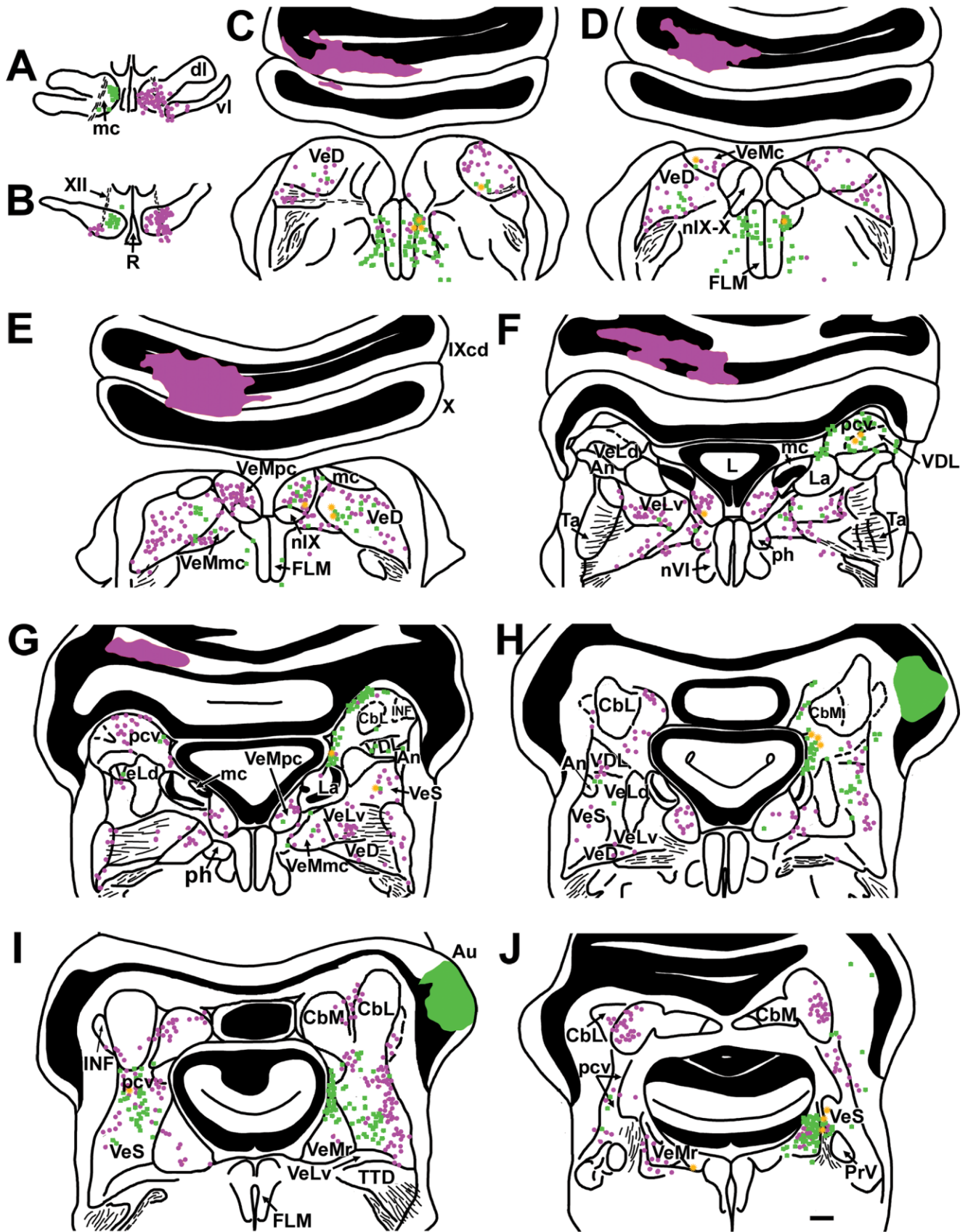


Fig. 5. Retrograde labeling in the vestibular nuclei, cerebellar nuclei, and reticular formation from injections in the ventral uvula and flocculus. Drawings of coronal sections illustrate the extent of the injection site (C–J, red and green shading), the labeling in the inferior olive (A,B), and the extent and distribution of labeling in the vestibular and cerebellar nuclei (C–J). Each dot represents the location of a retrogradely labeled cell and is color-coded to the injection site (green squares and red circles; the “red” injection and labeled cells have been

pseudocoloured magenta to accommodate readers with red-green color blindness). Double-labeled cells obtained from the adjacent section are shown as orange stars. The green injection was confined to the right flocculus. The red injection was primarily in the ventral uvula on the left side but crossed the midline and extended laterally to encroach upon the left flocculus. C–J are approximately 400 μ m apart. For abbreviations, see list. Scale bar = 1 mm in J (applies to A–J).

1992; Wylie et al., 1999b; Pakan et al., 2005). Despite the striking similarity of the flocculus in birds and mammals, the same cannot be said of the uvula-nodulus. We must caution that a direct comparison between the present study and previous mammalian studies may not be entirely appropriate because of differences with respect to the uvula-nodulus. In pigeons, the uvula-nodulus is distinguished by Purkinje cell CSA that responds best to patterns of translational optic flow (Wylie et al., 1993, 1998; Wylie and Frost, 1999). However, in rabbits, Purkinje cell CSA responds best to either rotational optic flow or head tilt originating in the otolith organs (Shojaku et al., 1991; Barmack and Shojaku, 1992, 1995).

Yakusheva et al. (2007) recently recorded Purkinje cell activity in the uvula-nodulus of monkeys during tilt, translation, and their combinations, as well as during earth-vertical and earth-horizontal axis rotations. Their data suggested that most cells encode translational motion rather than net gravito-inertial acceleration. Thus, although there is similarity between the pigeon and mammalian uvula-nodulus with respect to processing translational motion, the species similarities are not as striking as for the flocculus. Moreover, in mammals it is clear that there are differences between the uvula and nodulus with respect to mossy fiber input (see Voogd and Barmack, 2006 for review).

Surprisingly, we found relatively few labeled cells in the ph from our injections. In mammals, the ph provides al-

most 20% of the mossy fiber input to the flocculus and is on the order of 5–20% to the uvula and nodulus (Akaogi et al., 1994; Ruigrok, 2003). A cerebellar projection from the presumed homologue of the eph has also been reported in the developing frog (van der Linden and ten Donkelaar, 1987).

Although we did not offer an exhaustive description of projections from the reticular formation, the density of labeling caudally in the region of the FLM from flocculus injections was impressive. After injections into the uvula-nodulus, labeling in this region was sparse. Ruigrok (2003) also noted that the projection from “MLF neurons” was twice as heavy to the flocculus compared with the nodulus. These neurons likely correspond to the paramedian tract (PMT) neurons described by Büttner-Ennever, Horn, and colleagues (Büttner-Ennever et al., 1989; Büttner-Ennever, 1992; Büttner-Ennever and Horn, 1996; Horn, 2006). PMT neurons are described as lying “slightly lateral within the fibers of paramedian tracts” (Horn, 2006), which matches the description of those cells observed in the present study. In mammals there are several PMT groups that project to the flocculus scattered rostro-caudally within the FLM from the level of the abducens nucleus to the hypoglossal nucleus. The cells we observed in this region do not appear to reside in distinct clusters, and most were well caudal to the abducens nucleus but did not extend as far caudal as the hypoglossal nucleus. Thus these cells may be homologous to the mid-caudal PMT groups such as the nucleus paraphales (Horn, 2006).

Comparison with efferent projections of the vestibulocerebellum

Wylie et al. (1999a) investigated the projections of Purkinje cells in the flocculus vs. uvula-nodulus in pigeon (see also Wylie et al., 2003a,b). Purkinje cells project exclusively to the vestibular and cerebellar nuclei on the ipsilateral side of the brain. In the present study we found that the vestibular and cerebellar nuclei project bilaterally to the uvula-nodulus, with approximately equal weight from the ipsilateral and contralateral sides. The projection to the flocculus is also bilateral, although much heavier from the ipsilateral side (2:1). These projections are summarized in Figure 6B along with the results of the present study (Fig. 6A) to allow a direct comparison of the Purkinje cell efferents and mossy fiber afferents of the uvula-nodulus (blue) and flocculus (yellow). The projections of the different regions of the VbC to the vestibular

TABLE 4. Number of Double-Labeled Cells From Injections of Red and Green Microspheres in the Flocculus on Opposite Sides of the Brain¹

	Fl+Fl#3		Fl+Fl#5	
	No. of double-labeled cells (lower count)		No. of double-labeled cells (lower count)	
VeM	17 (178)		1 (105)	
VeS	13 (85)		2 (56)	
pcv	3 (49)		2 (69)	
VeLv	1 (10)		0 (1)	
VeD	12 (92)		1 (40)	
VDL/INF	0 (4)		0 (5)	
Ph	6 (21)		5 (14)	
CbM	0 (3)		0 (2)	
CbL	0 (0)		0 (0)	
PMA	2 (36)		11 (63)	
Total	54 (478) = 11.3%		22 (355) = 6.2%	

¹So that this can be expressed as a proportion, the lower of the total number of neurons in a given nucleus from the two injections is indicated in parentheses. For abbreviations, see list.

TABLE 5. Number of Double-Labeled Cells From Injections of Red and Green Microspheres in the Flocculus and Ventral Uvula¹

	Fl+UVN#2		Fl+UVN#4		Fl+UVN#1	
	No. of double-labeled cells (lower count)		No. of double-labeled cells (lower count)		No. of double-labeled cells (lower count)	
VeM	9 (120)		21 (150)		44 (200)	
VeS	2 (102)		3 (45)		35 (157)	
pcv	6 (104)		7 (59)		25 (126)	
VeLv	0 (6)		1 (2)		0 (2)	
VeD	6 (70)		7 (73)		25 (126)	
VDL/INF	2 (12)		2 (11)		3 (18)	
Ph	1 (20)		0 (6)		0 (2)	
CbM	0 (0)		0 (0)		1 (27)	
CbL	0 (0)		0 (0)		0 (0)	
PMA	12 (46)		1 (69)		3 (19)	
Total	38 (600) = 6.3%		42 (565) = 7.4%		136 (867) = 15.7%	

¹So that this can be expressed as a proportion, the lower of the total number of neurons in a given nucleus from the two injections is indicated in parentheses. For abbreviations, see list.

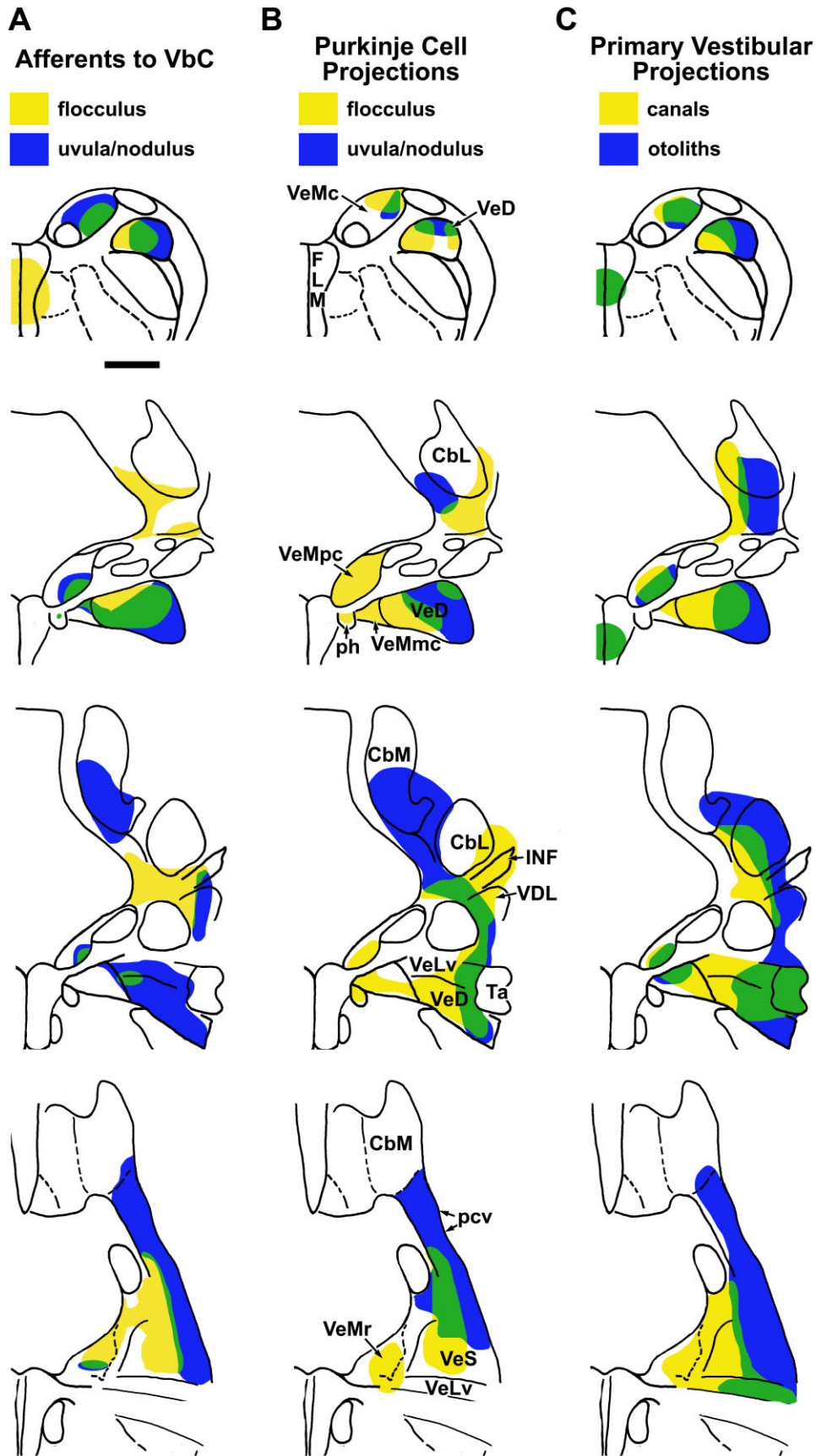


Fig. 6. A schematic summary of the distribution of afferents and efferents of the vestibular nuclei, compiled from the present study and indicated on idealized coronal sections from Karten and Hodos (1967). **A:** Projections of the vestibular nuclei to either the flocculus (yellow), the uvula-nodulus (blue), or both (green). **B:** Projections from the flocculus and uvula-nodulus, as compiled from Wylie et

al. (1999a, 2003a, b). **C:** The primary vestibular projections (semicircular canals, yellow; otoliths, blue; semicircular canals and otoliths, green) to these areas are indicated, as gleaned from Dickman and Fang (1996) and Schwarz and Schwarz (1986). For abbreviations see list. Scale bar = 1 mm in A (applies to A-C).

nuclei are largely distinct, with some overlap. Also, the distributions of the mossy fiber afferents mirror those of the Purkinje cell efferents in several, but certainly not all, respects. With respect to the VeD, there is a complementary but overlapping pattern such that the medial VeD receives more input from the flocculus, whereas the lateral VeD receives input from the uvula-nodulus. Concerning the vestibular input to the VbC, this is similar to what was observed in the present study.

With respect to the VeS, the projection of the flocculus was to the dorsal, medial, and central parts of the VeS, but that from the uvula-nodulus was directed more laterally. This pattern corresponds well with the distribution of vestibular neurons projecting to these zones as reported in the present study. Other aspects also display congruence of cerebellar afferents and efferents. The flocculus more so than the uvula-nodulus is associated with the rostral part of the VeM and the caudal parts of the pcv in the vicinity of CbL, whereas the CbM, and the rostral pcv surrounding the CbM are more associated with the uvula-nodulus.

Comparison with the primary vestibular projection

The semicircular canals are sensitive to rotation of the head, whereas the otolith organs respond to the linear acceleration that would result from self-translation (Wilson and Melvill Jones, 1979). Thus one might hypothesize that the canals and otolith organs project to those areas of the vestibular and cerebellar nuclei receiving input from Purkinje cells and projecting to the granule cell layer in the flocculus (rotation) and uvula-nodulus (translation), respectively. Detailed descriptions of the projections of the vestibular apparatus have been provided by Schwarz and Schwarz (1986) and Dickman and Fang (1996), and their findings do support the above stated hypothesis to some degree, as illustrated in Figure 6C. The projection to the VeS is to the dorsal and medial aspects from the canals and to the dorsal and lateral margins from the otoliths. Likewise, we found that the lateral margin of the VeS projected more heavily to the uvula-nodulus, and the medial margin projected more heavily to the flocculus. Although this indicates that the areas of the VeS receiving input from canals and otoliths project to the flocculus and uvula-nodulus, respectively, this should be taken as a generality rather than a strict concordance. For example, from flocculus injections the labeling in the contralateral VeS is slightly more lateral (Fig. 2F) and overlaps with the region that projects to the uvula-nodulus (e.g., Fig. 5J). This implies that the flocculus might be receiving secondary otolith input from the contralateral VeS.

Schwarz and Schwarz (1986) found that the projection to the VeD was largely to the medial half from the canals and to the lateral half from the otolith organs. Similarly, we found that the medial and lateral halves of the VeD projected most heavily to the granule cell layer in the flocculus and uvula-nodulus, respectively. The VeM receives input from both the canals and the otoliths. Dickman and Fang (1996) suggested that although the projections were overlapping, the canals projected more medially than the otoliths. The VeMr, which we showed provides a major input to the ipsilateral flocculus, receives input from both the canals and the otoliths (Schwarz and Schwarz, 1986; Dickman and Fang, 1996).

With respect to the cerebellar nuclei, Dickman and Fang (1996) reported that the projection from the canals was largely to the CbL, whereas the projection of the otoliths was to the lateral margin of the CbM and CbL. We found that there was a projection to the uvula-nodulus from the lateral and ventral regions of the CbM, which would be expected; however, we did not find any significant amount of retrograde labeling in either the CbM or CbL from the flocculus injections.

In summary, we conclude that the flocculus receives secondary vestibular information mainly from the semicircular canals, whereas the uvula-nodulus receives secondary vestibular information mainly from the otolith organs. Clearly this is a generalization, as there is canal-otolith convergence in the many areas in the vestibular nuclei receiving both otolith and canal input. Moreover, the primary vestibular projection to the flocculus and the uvula-nodulus in pigeons arises from both the canals and the otolith organs. As Yakusheva et al. (2007) have shown, canal-otolith convergence is necessary to encode translation unambiguously. The otolith organs respond to linear acceleration due to head tilt or translation of the head. Head tilt also results in activation of canal afferents, whereas translation of the head does not. Yakusheva et al. (2007) showed that Purkinje cells in the uvula-nodulus in monkeys respond to translation but not head tilt. However, if the canals are deactivated by plugging, the uvula-nodulus cells respond equally well to tilt and translation. Thus, the canal input is necessary for distinguishing head tilt from translation.

Consideration with respect to eye movement and head movement control

Generally speaking, the flocculus has been tightly linked to the generation of compensatory eye movement control (e.g., Voogd and Barmack, 2006) but has a lesser role in head movement control (De Zeeuw and Koekkoek, 1997). CSA in the flocculus responds to optic flow induced by head rotation, which could be compensated for by rotational eye and head movements (Gioanni, 1988). The uvula-nodulus seems to have some role in eye movement behaviour, but rather is associated with axial musculature and the control of posture and movement (Voogd and Barmack, 2006). CSA in the medial VbC responds to optic flow induced by self-translation, which would be compensated for by translatory head and/or body movements, such as the stereotypical head-bobbing seen in pigeons (Friedman, 1975; Frost, 1978; Nalbach, 1992). In monkeys, translational radial flow elicits vergence eye movements (Kodaka et al., 2007), but this has not been shown in pigeons or other lateral-eyed species. Given the physiological response properties of Purkinje cells in the flocculus and uvula-nodulus, one would expect that both the flocculus and uvula-nodulus would be associated with descending projections to the spinal cord for control of head movement, whereas the flocculus, more so than the uvula-nodulus, would be associated with ascending projections to oculomotor structures. Wylie et al. (2003a,b) showed that with respect to Purkinje cell projections of the flocculus vs. the uvula-nodulus, this is generally the case. The present paper shows that the vestibular-VbC projection also supports this pattern.

The central and medial parts of the VeS, which project to the flocculus (present study), are heavily labeled after injections into the oculomotor and trochlear nuclei (Wold,

1978; Labandeira-Garcia et al., 1989; Arends et al., 1991). Mammalian studies indicate that this projection is highly conserved (see Highstein and Holstein, 2006 for review). In contrast, the lateral VeS and CbM, which were labeled after injections into the uvula-nodulus in the present study, are also labeled after injections into the cervical spinal cord (Arends et al., 1991). From oculomotor nuclei injections, Labandeira-Garcia et al. (1989) and Wold (1978) also noted retrogradely labeled neurons medial to the VeS, which they ascribed to cell group A. These could correspond to the neurons in the wall of the 4th ventricle that we observed from flocculus injections in the present study. Labandeira-Garcia et al. (1989) found that a region dorsal to nuclei angularis was heavily labeled after injection into the oculomotor nuclei. Their drawings indicate that this is the same area in which we saw dense labeling after injections in the flocculus (the caudal VDL and vicinity). They ascribed these neurons to the VDL and noted that it might be homologous to the oculomotor projection of the y group in mammals (see Highstein and Holstein, 2006 for review). However, Arends et al. (1991) found that the VDL projects to the spinal cord and the abducens nucleus, whereas there was a heavy projection from the Inf to the oculomotor and trochlear nuclei. Both the flocculus and the uvula-nodulus also receive input from the VeD and VeM (present study), which have both oculomotor and collimator projections (Wold, 1978; Labandeira-Garcia et al., 1989; Arends et al., 1991). However, at this point it is not clear whether the VeD and VeM pools projecting to the flocculus vs. uvula-nodulus have differential ascending and descending projections.

Conclusions

In the present study we have shown that in pigeons, the flocculus, which is involved in processing rotational optic flow, and the uvula-nodulus, which is involved in the processing of translational optic flow, have differential mossy fiber inputs from the vestibular and associated nuclei. Given that the flocculus and uvula-nodulus are composed of multiple zones themselves (Wylie et al., 2003b; Voogd and Wylie, 2004), it is not unlikely that there are differential projections from the vestibular and associated nuclei to these zones within the flocculus and uvula-nodulus. Generally speaking, those areas of the vestibular nuclei that project to the flocculus also receive input from the flocculus and semicircular canals, whereas the areas of the vestibular nuclei that project to the uvula-nodulus receive input from the uvula-nodulus and otolith organs. Finally, again generally speaking, those areas that project to the flocculus are associated with ascending projections to the oculomotor nuclei and descending projections to the spinal cord, whereas those areas that project to the uvula-nodulus are associated with descending projections to the spinal cord rather than ascending projections to the oculomotor nuclei.

LITERATURE CITED

- Akaogi K, Sato Y, Ikarashi K, Kawasaki T. 1994. Mossy fiber projections from the brain stem to the nodulus in the cat. An experimental study comparing the nodulus, the uvula and the flocculus. *Brain Res* 638:12–20.
- Arends J, Voogd J. 1989. Topographic aspects of the olivocerebellar system in the pigeon. *Exp Brain Res* 17(Suppl):52–57.
- Arends JJ, Zeigler HP. 1991. Organization of the cerebellum in the pigeon (*Columba livia*): I. Corticonuclear and corticovestibular connections. *J Comp Neurol* 306:221–244.
- Arends JJ, Allan RW, Zeigler HP. 1991. Organization of the cerebellum in the pigeon (*Columba livia*): III. Corticovestibular connections with eye and neck premotor areas. *J Comp Neurol* 306:273–289.
- Barmack NH, Shojaku H. 1992. Vestibularly induced slow oscillations in climbing fiber responses of Purkinje cells in the cerebellar nodulus of the rabbit. *Neuroscience* 50:1–5.
- Barmack NH, Shojaku H. 1995. Vestibular and visual climbing fiber signals evoked in the uvula-nodulus of the rabbit cerebellum by natural stimulation. *J Neurophysiol* 74:2573–2589.
- Brecha N, Karten HJ, Hunt SP. 1980. Projections of the nucleus of the basal optic root in the pigeon: an autoradiographic and horseradish peroxidase study. *J Comp Neurol* 189:615–670.
- Büttner-Ennever JA. 1992. Patterns of connectivity in the vestibular nuclei. *Ann N Y Acad Sci* 656:363–378.
- Büttner-Ennever JA. 1999. A review of otolith pathways to brainstem and cerebellum. *Ann N Y Acad Sci* 871:51–64.
- Büttner-Ennever JA. 2000. Overview of the vestibular system: Anatomy. Beitz A, Anderson J, editors: CRC Press LLC, Boca Raton, FL. 3–24 p.
- Büttner U, Büttner-Ennever JA. 2006. Present concepts of oculomotor organization. *Prog Brain Res* 151:1–42.
- Büttner-Ennever JA, Horn AK. 1996. Pathways from cell groups of the paramedian tracts to the floccular region. *Ann N Y Acad Sci* 781:532–540.
- Büttner-Ennever JA, Horn AK, Schmidtke K. 1989. Cell groups of the medial longitudinal fasciculus and paramedian tracts. *Rev Neurol (Paris)* 145:533–539.
- Carleton SC, Carpenter MB. 1983. Afferent and efferent connections of the medial, inferior and lateral vestibular nuclei in the cat and monkey. *Brain Res* 278:29–51.
- Cox RG, Peusner KD. 1990. Horseradish peroxidase labeling of the efferent and afferent pathways of the avian tangential vestibular nucleus. *J Comp Neurol* 296:324–341.
- Crowder NA, Winship IR, Wylie DR. 2000. Topographic organization of inferior olive cells projecting to translational zones in the vestibulocerebellum of pigeons. *J Comp Neurol* 419:87–95.
- De Zeeuw CI, Koekkoek SK. 1997. Signal processing in the C2 module of the flocculus and its role in head movement control. *Prog Brain Res* 114:299–320.
- Diaz C, Puelles L. 2003. Plurisegmental vestibulocerebellar projections and other hindbrain cerebellar afferents in midterm chick embryos: biotinylated dextranamine experiments in vitro. *Neuroscience* 117:71–82.
- Diaz C, Glover JC, Puelles L, Bjaalie JG. 2003. The relationship between hodological and cytoarchitectonic organization in the vestibular complex of the 11-day chicken embryo. *J Comp Neurol* 457:87–105.
- Dickman JD, Fang Q. 1996. Differential central projections of vestibular afferents in pigeons. *J Comp Neurol* 367:110–131.
- Epema AH, Gerrits NM, Voogd J. 1988. Commissural and intrinsic connections of the vestibular nuclei in the rabbit: a retrograde labeling study. *Exp Brain Res* 71:129–146.
- Epema AH, Gerrits NM, Voogd J. 1990. Secondary vestibulocerebellar projections to the flocculus and uvulonodular lobule of the rabbit: a study using HRP and double fluorescent tracer techniques. *Exp Brain Res* 80:72–82.
- Friedman MB. 1975. Visual control of head movements during avian locomotion. *Nature* 255:67–69.
- Frost BJ. 1978. Moving background patterns alter directionally specific responses of pigeon tectal neurons. *Brain Res* 151:599–603.
- Gibson JJ. 1954. The visual perception of objective motion and subjective movement. *Psychol Rev* 61:304–314.
- Gioanni H. 1988. Stabilizing gaze reflexes in the pigeon (*Columba livia*). I. Horizontal and vertical optokinetic eye (OKN) and head (OCR) reflexes. *Exp Brain Res* 69:567–582.
- Graf W, Simpson JI, Leonard CS. 1988. Spatial organization of visual messages of the rabbit's cerebellar flocculus. II. Complex and simple spike responses of Purkinje cells. *J Neurophysiol* 60:2091–2121.
- Highstein SM, Holstein GR. 2006. The anatomy of the vestibular nuclei. *Prog Brain Res* 151:157–203.
- Horn AK. 2006. The reticular formation. *Prog Brain Res* 151:127–155.
- Karten H, Hodós W. 1967. A stereotaxic atlas of the brain of the pigeon (*Columba livia*). Baltimore: Johns Hopkins Press.

- Kevetter GA, Perachio AA. 1986. Distribution of vestibular afferents that innervate the sacculus and posterior canal in the gerbil. *J Comp Neurol* 254:410–424.
- Kodaka Y, Sheliga BM, Fitzgibbon EJ, Miles FA. 2007. The vergence eye movements induced by radial optic flow: some fundamental properties of the underlying local-motion detectors. *Vision Res* 47:2637–2660.
- Labandeira-Garcia JL, Guerra-Seijas MJ, Labandeira-Garcia JA, Jorge-Barreiro FJ. 1989. Afferent connections of the oculomotor nucleus in the chick. *J Comp Neurol* 282:523–534.
- Larsell O. 1967. The cerebellum: from myxinooids through birds. Jansen J, editor. MN: The University of Minnesota Press.
- Lau KL, Glover RG, Linkenhoker B, Wylie DR. 1998. Topographical organization of inferior olive cells projecting to translation and rotation zones in the vestibulocerebellum of pigeons. *Neuroscience* 85:605–614.
- Nalbach HO. 1992. Translational head movements of pigeons in response to a rotating pattern: characteristics and tool to analyse mechanisms underlying detection of rotational and translational optical flow. *Exp Brain Res* 92:27–38.
- Newlands SD, Perachio AA. 2003. Central projections of the vestibular nerve: a review and single fiber study in the Mongolian gerbil. *Brain Res Bull* 60:475–495.
- Pakan JM, Todd KG, Nguyen AP, Winship IR, Hurd PL, Jantzie LL, Wylie DR. 2005. Inferior olivary neurons innervate multiple zones of the flocculus in pigeons (*Columba livia*). *J Comp Neurol* 486:159–168.
- Purcell IM, Perachio AA. 2001. Peripheral patterns of terminal innervation of vestibular primary afferent neurons projecting to the vestibulocerebellum in the gerbil. *J Comp Neurol* 433:48–61.
- Ruigrok TJ. 2003. Collateralization of climbing and mossy fibers projecting to the nodulus and flocculus of the rat cerebellum. *J Comp Neurol* 466:278–298.
- Ruigrok TJ, Osse RJ, Voogd J. 1992. Organization of inferior olivary projections to the flocculus and ventral paraflocculus of the rat cerebellum. *J Comp Neurol* 316:129–150.
- Sato Y, Kawasaki T. 1987. Organization of maculo-ocular pathways via y-group nucleus and its relevance to cerebellar flocculus in cats. *Physiologist* 30(1 Suppl):S77–80.
- Schwarz DW, Schwarz IE. 1986. Projection of afferents from individual vestibular sense organs to the vestibular nuclei in the pigeon. *Acta Otolaryngol* 102:463–473.
- Schwarz IE, Schwarz DW. 1983. The primary vestibular projection to the cerebellar cortex in the pigeon (*Columba livia*). *J Comp Neurol* 216:438–444.
- Shojaku H, Barmack NH, Mizukoshi K. 1991. Influence of vestibular and visual climbing fiber signals on Purkinje cell discharge in the cerebellar nodulus of the rabbit. *Acta Otolaryngol Suppl* 481:242–246.
- Straka H, Baker R, Gilland E. 2001. Rhombomeric organization of vestibular pathways in larval frogs. *J Comp Neurol* 437:42–55.
- Straka H, Holler S, Goto F. 2002. Patterns of canal and otolith afferent input convergence in frog second-order vestibular neurons. *J Neurophysiol* 88:2287–2301.
- Tan J, Gerrits NM, Nanhoe R, Simpson JI, Voogd J. 1995. Zonal organization of the climbing fiber projection to the flocculus and nodulus of the rabbit: a combined axonal tracing and acetylcholinesterase histochemical study. *J Comp Neurol* 356:23–50.
- ten Donkelaar H. 1998. Reptiles. In: Nieuwenhuys R, ten Donkelaar HJ, Nicholson C, editors. The central nervous system. Berlin Springer-Verlag. p 1315–1511.
- van der Linden JA, ten Donkelaar HJ. 1987. Observations on the development of cerebellar afferents in *Xenopus laevis*. *Anat Embryol (Berl)* 176:431–439.
- Voogd J, Barmack NH. 2006. Oculomotor cerebellum. *Prog Brain Res* 151:231–268.
- Voogd J, Wylie DR. 2004. Functional and anatomical organization of floccular zones: a preserved feature in vertebrates. *J Comp Neurol* 470:107–112.
- Voogd J, Gerrits NM, Ruigrok TJ. 1996. Organization of the vestibulocerebellum. *Ann N Y Acad Sci* 781:553–579.
- Wild JM, Karten HJ, Frost BJ. 1993. Connections of the auditory forebrain in the pigeon (*Columba livia*). *J Comp Neurol* 337:32–62.
- Wilson J, Melvill Jones G. 1979. Mammalian vestibular physiology. New York: Plenum Press.
- Winship IR, Wylie DR. 2003. Zonal organization of the vestibulocerebellum in pigeons (*Columba livia*): I. Climbing fiber input to the flocculus. *J Comp Neurol* 456:127–139.
- Winship IR, Wylie DR. 2006. Receptive-field structure of optic flow responsive Purkinje cells in the vestibulocerebellum of pigeons. *Vis Neurosci* 23:115–126.
- Wold JE. 1976. The vestibular nuclei in the domestic hen (*Gallus domesticus*). I. Normal anatomy. *Anat Embryol (Berl)* 149:29–46.
- Wold JE. 1978. The vestibular nuclei in the domestic hen (*Gallus domesticus*). IV. The projection to the spinal cord. *Brain Behav Evol* 15:41–62.
- Wylie DR, Frost BJ. 1993. Responses of pigeon vestibulocerebellar neurons to optokinetic stimulation. II. The 3-dimensional reference frame of rotation neurons in the flocculus. *J Neurophysiol* 70:2647–2659.
- Wylie DR, Frost BJ. 1999. Complex spike activity of Purkinje cells in the ventral uvula and nodulus of pigeons in response to translational optic flow. *J Neurophysiol* 81:256–266.
- Wylie DR, Kripalani T, Frost BJ. 1993. Responses of pigeon vestibulocerebellar neurons to optokinetic stimulation. I. Functional organization of neurons discriminating between translational and rotational visual flow. *J Neurophysiol* 70:2632–2646.
- Wylie DR, Bischof WF, Frost BJ. 1998. Common reference frame for neural coding of translational and rotational optic flow. *Nature* 392:278–282.
- Wylie DR, Lau KL, Lu X, Glover RG, Valsangkar-Smyth M. 1999a. Projections of purkinje cells in the translation and rotation zones of the vestibulocerebellum in pigeon (*Columba livia*). *J Comp Neurol* 413:480–493.
- Wylie DR, Winship IR, Glover RG. 1999b. Projections from the medial column of the inferior olive to different classes of rotation-sensitive Purkinje cells in the flocculus of pigeons. *Neurosci Lett* 268:97–100.
- Wylie DR, Brown MR, Barkley RR, Winship IR, Crowder NA, Todd KG. 2003a. Zonal organization of the vestibulocerebellum in pigeons (*Columba livia*): II. Projections of the rotation zones of the flocculus. *J Comp Neurol* 456:140–153.
- Wylie DR, Brown MR, Winship IR, Crowder NA, Todd KG. 2003b. Zonal organization of the vestibulocerebellum in pigeons (*Columba livia*): III. Projections of the translation zones of the ventral uvula and nodulus. *J Comp Neurol* 465:179–194.
- Yakusheva TA, Shaikh AG, Green AM, Blazquez PM, Dickman JD, Angelaki DE. 2007. Purkinje cells in posterior cerebellar vermis encode motion in an inertial reference frame. *Neuron* 54:973–985.